# Self-Localization of Polariton Condensates in Periodic Potentials

E. A. Ostrovskaya,[1] J. Abdullaev,[1] M. D. Fraser,[2] A. S. Desyatnikov,[1] and Yu. S. Kivshar[1]

[1]*Nonlinear Physics Centre, Research School of Physics and Engineering, The Australian National University, Canberra ACT 0200, Australia*

[2]*National Institute of Informatics, 2-1-2 Hitotsubashi, Chiyoda-ku, Tokyo 101-8430, Japan*

(Received 10 October 2012; published 26 April 2013)

We predict the existence of novel spatially localized states of exciton-polariton Bose-Einstein condensates in semiconductor microcavities with fabricated periodic in-plane potentials. Our theory shows that, under the conditions of continuous nonresonant pumping, localization is observed for a wide range of optical pump parameters due to effective potentials self-induced by the polariton flows in the spatially periodic system. We reveal that the self-localization of exciton-polaritons in the lattice may occur both in the gaps and bands of the single-particle linear spectrum, and is dominated by the effects of gain and dissipation rather than the structured potential, in sharp contrast to the conservative condensates of ultracold alkali atoms.

DOI: 10.1103/PhysRevLett.110.170407 PACS numbers: 05.30.Jp, 03.75.Kk, 03.75.Lm, 71.36.+c

*Introduction.*—Ultracold atomic gases loaded into periodic ''lattice'' potentials provide a fascinating tool for exploring fundamental quantum many-body physics, as well as offering an opportunity to build quantum simulators and scalable quantum information processing systems [1].

In recent years, polariton condensates created in semiconductor microcavities [2] have emerged as an attractive alternative to the atomic Bose-Einstein condensates (BECs), owing to the relatively high condensation temperatures, direct momentum and real-space imaging via the cavity photoluminescence, and possibility to manipulate condensates using both optical pump and structure of the microcavity [3]. Considerable effort has been directed towards achieving the polariton condensation in lattice potentials and observing macroscopic population of the single-particle band-gap spectrum. So far, the majority of the experiments with exciton-polaritons in periodic potentials have been performed in a pulsed excitation regime, which has allowed us to populate and image rapidly decaying high momentum states. The staggered ''$\pi$-state'' higher-order Bloch states have been demonstrated in a one-dimensional (1D) lattice created by metal deposition onto the microcavity [4]. Similarly, condensation into the second band has been achieved in a two-dimensional (2D) square lattice [5], and the Brillouin zone structure of the kagome lattice has been mapped out [6]. Recently, condensation into an energy state corresponding to a spectral gap has been demonstrated in a 1D lattice created by modulation of quantum wires in a microcavity [7]. Condensation in tunable acoustically created lattices has also been investigated [8,9].

One of the fundamental effects due to the band-gap structure is localization of the condensate in real space. In kagome lattices [6] this could be achieved via dispersionless dynamics in the flat spectral band. Alternatively, spatial localization in spectral gaps of the band-gap structure can be achieved through the balance of repulsive nonlinearity and modified effective dispersion due to the negative effective mass. This mechanism has been explored in the context of gap solitons in photonic [10] and matter-wave [11] band-gap structures. Scarce theoretical descriptions of exciton-polaritons in periodic potentials so far either attributed localization phenomena to intrinsic structural disorder [12] or disregarded the driven-dissipative nature of the polariton condensate arising due to finite lifetime of quasiparticles and the presence of the optical pump [13,14]. This distinct nature of polariton condensates becomes especially important in the continuous-wave (cw) nonresonant excitation regime [2], which creates condensates with spontaneously established spatial coherence and long coherence times. The gain-assisted localization and related dynamics plays a critical role for such condensates [15,16], in contrast to atomic BECs in thermal equilibrium.

In this Letter, we identify and analyze the mechanism for localization of a dissipative polariton condensate in a fabricated periodic potential under incoherent cw excitation. We show that the driven-dissipative nature of the polariton condensate gives rise to effective potentials local to the condensate, namely a defect-type potential introduced by the pump-induced polariton reservoir and a potential self-induced by the strongly modulated flow of polaritons away from the excitation spot. Trapping of the polariton condensate in these effective potentials, which supersede the external lattice potential, is responsible for its spatial localization.

*Model.*—We assume that a near-equilibrium polariton condensate is formed via cw incoherent excitation with a spatially inhomogeneous optical pump. Above condensation threshold, it can be described by the mean field open-dissipative model for a polariton condensate coupled to an incoherent polariton reservoir density [17],

 

$$i\frac{\partial\Psi}{\partial t} = \left[-\frac{\nabla_\perp^2}{2} + V_{NL} + \frac{i}{2}(Rn_R - \gamma_c) + V_L\right]\Psi, \qquad (1)$$
$$\frac{\partial n_R}{\partial t} = -(\gamma_R + R|\Psi|^2)n_R(\vec{r}, t) + P(\vec{r}).$$

Here $\Psi$ is the condensate wave function, $V_L(\vec{r})$ is a periodic potential experienced by the polaritons, and $V_{NL} = g_c|\Psi|^2 + g_R n_R$ is an effective nonlinear potential depending both on the condensate density and the reservoir density, $n_R$, which is determined by the pump $P(\vec{r})$. Parameters defining the condensate dynamics are the relaxation rates of the condensed polaritons $\gamma_c$ and reservoir polaritons $\gamma_R$, the stimulated scattering rate $R$, and the polariton-polariton interaction strengths $g_R$, $g_c$. Equation (1) is written in the dimensionless form by using the characteristic scaling units of time $1/\gamma_c$, energy $\hbar\gamma_c$, and length $[\hbar/(m_{LP}\gamma_c)]^{1/2}$, where $m_{LP}$ is the lower-polariton effective mass [18]. Under this scaling $\gamma_c = 1$; however, we formally retain this parameter hereafter. The scaling units are calculated using the parameters close to those of the experimental setup of [19], with $m_{\mathrm{LP}} = 10^{-3}m_e$, $g_c = 6 \times 10^{-3}$ meV $\mu$m$^2$, $g_R = 2g_c$, $\gamma_c = 0.02$ ps$^{-1}$, $\gamma_R = 1.5\gamma_c$, and $R = 0.01$ $\mu$m$^2$ ps$^{-1}$.

*1D localization.*—First, we consider the simplest model of a quasi-one-dimensional polariton condensate (e.g., confined in a microwire [20]) subject to a periodic potential approximated by a harmonic function $V_{\mathrm{L}}(x) = V_0\sin^2(k_l x)$, with the lattice constant $a = \pi/k_l$. Periodicity of the potential imposes a band-gap structure onto the lower polariton (LP) dispersion branch [4], and we can consider population of this band-gap structure by polaritons depending on the pump parameters. To this end, we look for the steady state solutions $\Psi(x) = \psi(x)\exp(iEt)$ of Eq. (1) governed by the complex Ginzburg-Landau equation. We assume the Gaussian pump profile $P(x) = P_0\exp(-\sigma^2x^2)$ and relate its peak intensity to the homogeneous threshold intensity $P_{\mathrm{th}} = \gamma_R\gamma_c/R$ [17].

As has been established both experimentally (see, e.g., [15,20]) and theoretically [16,18,21], nonresonant cw pump leads to spatial localization of polariton BEC even without a trapping potential. This effect, resulting in formation of dissipative solitons [18,22] is due to the balance of gain and loss in the system, and is dramatically different from formation of bright solitons in the coherent fields due to conventional balance of nonlinearity and dispersion (diffraction). Below, we demonstrate how spatial localization of the condensate due to the balance between gain and loss is affected by a periodic potential.

*Narrow excitation.*—A spatially narrow pump $P(x)$ can target a single lattice site and therefore produce an on-site or off-site excitation. The peak of the off-site excitation spot can be arbitrarily offset from the minimum of the lattice potential. As can be seen from Eq. (1), in the case of the near-threshold pump intensity, $P_0/P_{\mathrm{th}} \sim 1$, nonlinear effects can be neglected. In this case, assuming a straightforward balance of gain and loss, Eq. (1) would describe a condensate in the periodic potential $V_L(x)$ with the addition of a linear defect potential induced by the pump, $g_R n_R^0 \approx (g_R/\gamma_R)P(x)$, where $n_R^0 = P/(\gamma_R + R|\psi|^2)$ is the steady state reservoir density. The energy of the lowest-order defect modes is plotted as a function of pump intensity in Fig. 1, together with the band-gap spectrum imposed by the periodic potential.

Taking this spectrum as a frame of reference, we examine the energy and spatial structure of the localized steady state depending on the pump intensity. The respective dependence is plotted in Fig. 1 and shows that, for near-threshold on-site excitation, the energy of the localized state is indeed very close to that of a symmetric linear defect mode. As the ratio $P_0/P_{\mathrm{th}}$ grows, so does the energy of the localized state until it crosses into the band of the linear band-gap spectrum. This is in contrast to dissipative photonic lattice solitons [23] and defect states [24], which have been previously found to exist exclusively in the spectral gaps. An additional feature of the polariton steady states is transition, with growing pump intensity, from narrow states localized in a vicinity of a single potential well [Fig. 2(a)] to broader states with exponentially decaying and spatially modulated tails [Figs. 2(b) and 2(c)].

To understand the spatial structure of the localized states, we perform the Madelung transformation $\psi(x) = \sqrt{\rho(x)}\exp[i\phi(x)]$, and write down the steady state equations for the condensate density $\Phi = \sqrt{\rho}$ and phase gradient (flow velocity) $v = \phi_x$:

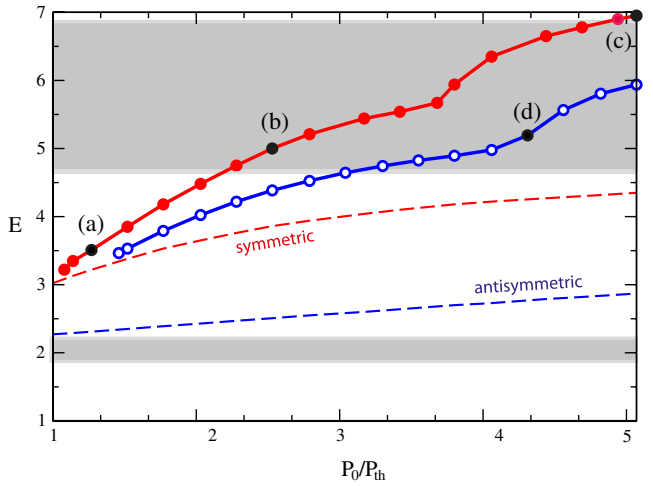


FIG. 1 (color online). Energy of the steady-state polariton condensate obtained with cw on-site (closed circles) or $\pi/4$ off-site (open circles) narrow Gaussian pump with the width $\sigma^2 = 0.6$. Shaded (open) areas show bands (gaps) of the single-particle Bloch-wave spectrum in the lattice potential $V_L(x)(V_0 = 5.0, k_l = 1.5)$. Dashed lines are linear defect states in the combined effective potential $V_L(x) + g_R P(x)/\gamma_R$ (see text).

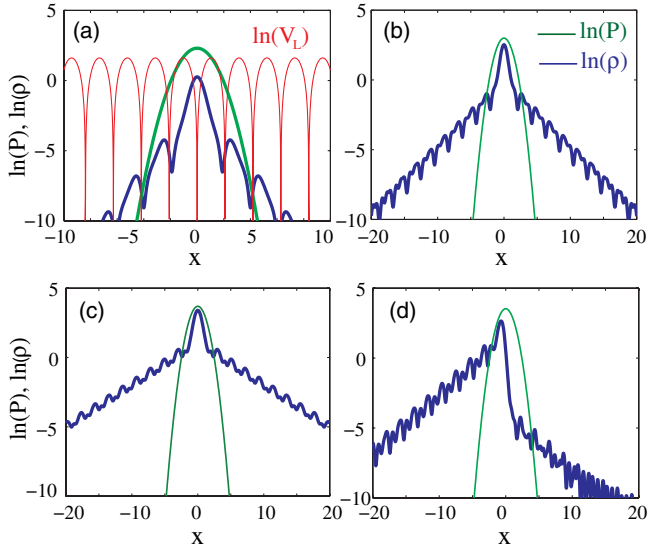


FIG. 2 (color online). Spatial profiles of the condensate density $\ln(\rho(x))$ and pump intensity $\ln(P(x))$ in the lattice potential $V_L(x)$ with $V_0 = 5.0$ and $k_l = 1.5$, corresponding to the peak pump intensity $P_0/P_{\rm th} = 1.27$ [point (a) in Fig. 1], $P_0/P_{\rm th} = 2.53$ [point (b)], $P_0/P_{\rm th} = 5.06$ [point (c)], and $P_0/P_{\rm th} = 4.30$ [point (d)]. Panel (a) also shows the lattice potential $\ln(V_L)$ (note the difference in $x$-scale).

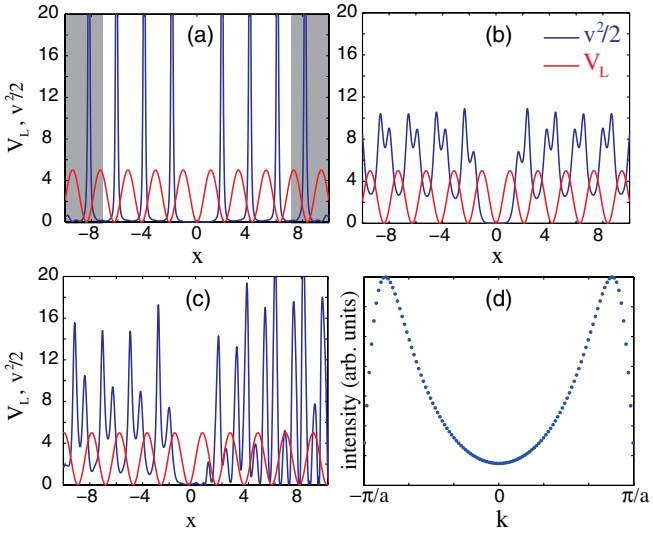


FIG. 3 (color online). Spatial profiles of the lattice potential $V_L(x)(V_0 = 5.0, k_l = 1.5)$ and the effective linear potential due to the phase gradient $v^2/2$ corresponding to the peak on-site pump intensities (a) $P_0/P_{\rm th} = 1.27$, (b) $P_0/P_{\rm th} = 5.06$, and (c) a noncentered pump ($\pi/4$ off site) with $P_0/P_{\rm th} = 4.30$. Panel (d) shows the $k$-space spectrum of the steady state [Fig. 2(a)] corresponding to the effective potential in (a).

$$\Phi_{xx} - 2\left(V_L + g_c\Phi^2 + g_R n_R^0 + \frac{v^2}{2}\right)\Phi + 2E\Phi = 0,$$
$$(\Phi^2 v)_x - (Rn_R^0 - \gamma_c)\Phi^2 = 0. \quad (2)$$

Given the rapid decay of the pump at large $x$, asymptotic behavior of the condensate near-linear density away from the pump spot is determined by the combination of the lattice potential $V_L(x)$ and a self-induced effective potential due to the phase gradient, $v^2(x)/2$. These two potentials for the narrow and wide states (a) and (b,c) in Figs. 1 and 2 are shown in Figs. 3(a)–3(c). The strong contribution of the Bloch states from the edges of the Brillouin zone into the composition of the localized state [Fig. 3(d)] leads to steep spatial gradients of the phase, $\phi(x)$. As a result, the flow of the condensate out of the excitation spot induces a periodic, tight-binding Kronig-Penney-like potential [Fig. 3(a)], and the band-gap spectrum due to the linear lattice potential becomes of little relevance to the energy eigenstates. The minima of the effective potential are offset from the minima of the lattice potential, which can cause the condensate density peaks to coincide with the maxima of the lattice potential [see Fig. 2(a)]. The tunnelling of the condensate out of the excitation spot is strongly inhibited by the tight-binding effective potential, until the modulations of the flow are smoothed out by the stronger pump. As demonstrated in Figs. 2(b) and 2(c), the strongly pumped condensate density extends over many wells of the periodic potential. In contrast to the lattice potential, the self-induced potential can become physically meaningless far on the tails of the condensate [shaded areas in Fig. 3(a)], where the density is negligible and any dynamical fluctuations can destroy regular phase structure.

Although the narrow gap states [Fig. 2(a)] resemble well localized gap solitons of a conservative BEC [11], they have no connection to the Bloch states at the band edge of the first Brillouin zone in the lattice potential, rather branching off the linear defect states. Their spatial extent is determined purely by the phase gradients established due to the balance of gain and loss in the system. The energy of the localized state can lie in either a spectral gap or band imposed by the lattice [25] since it is supported by the effective potentials created by the polariton flow and the role of the band-gap structure is diminished. Localization of in-band, as well as gap states, is strongly affected by the lattice potential modulating the flow, as illustrated in the Supplemental Material [25].

In the off-site excitation regime, the localized states can also be formed both within gaps and bands of the linear band-gap spectrum of the potential $V_L(x)$ [Fig. 1], and the threshold for the formation of these states is higher than that of the on-site state. Remarkably, the asymmetry of the defect created by the offset pump translates to the asymmetry of both the effective potential generated by the polariton flow and the condensate density [Figs. 2(d) and 3(c)]. Such asymmetric localized states are supported by the interface between two different effective potentials, and therefore resemble "mixed-gap" interface states of an atomic BEC in anharmonic lattices [26].

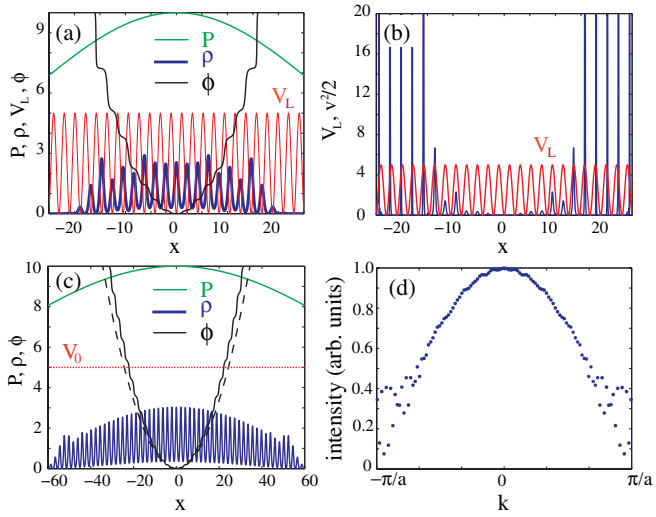


FIG. 4 (color online). (a),(c) Condensate density $\rho(x)$, phase $\phi(x)$, and lattice potential $V_L(x)(V_0 = 5.0, k_l = 1.5)$ corresponding to the peak on-site pump intensity $P_0/P_{\text{th}} = 1.27$ and widths $\sigma^2 = 6 \times 10^{-4}$ and $\sigma^2 = 6 \times 10^{-5}$, respectively. Dashed curve in (c) is the analytical approximation of $\phi(x)$ [Eq. (3)]. (b) Lattice potential $V_L$ and the self-induced potential, $v^2/2$, corresponding to (a). (d) Spectrum of the state (c) within the first Brillouin zone of the lattice potential.

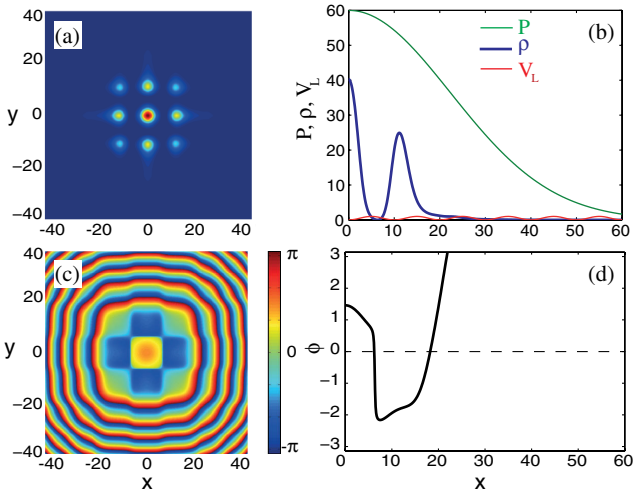


FIG. 5 (color online). Spatial profiles and cross-sections of the (a),(b) condensate density and (c),(d) phase, corresponding to a narrow in-gap state in a "square" lattice $V_L(x, y)(V_0 = 2.0, k_l = \pi/4)$.

*Wide excitation.*—By fixing the pump intensity and extending its width significantly beyond the single lattice well, we find a variety of spatially extended nearly energy-degenerate localized states. One example of such a gap state and its supporting effective potential is presented in Figs. 4(a) and 4(b). These states strongly resemble truncated nonlinear Bloch states in a conservative BEC [27]. However, the localization in this case is due to the effective potential created by the polariton flow out of the finite gain region.

A very wide, locally homogeneous, near-threshold pump generates extended states that locally resemble a ground Bloch state [Fig. 4(c)] of the lattice potential $V_L(x)$. In this regime, the asymptotic approximation of the phase profile at $x \to 0$, derived in [18] for the case of untrapped polariton condensate becomes valid for most of the excitation region [Fig. 4(c), dashed line], and the effective potential due to the polariton flow becomes harmonic,

$$v^2(x) \approx \frac{\gamma_c^2}{4}\left(\frac{P_0}{P_{\text{th}}} - 1\right)^2 x^2. \tag{3}$$

The density profile is a typical ground state supported by the combination of the periodic and harmonic effective potential [Fig. 4(c)], and its $k$-space spectrum [Fig. 4(d)] displays localization around $k = 0$ characteristic of the ground state in the lattice [4]. Thus, in this regime the dissipative condensate in a periodic potential mimics the behavior of a conservative condensate in the combined periodic and harmonic potentials.

*2D localization.*—Similarly to the 1D case, we find that excitation spots of varying width can create narrow and wide localized steady states of the polariton condensate both in the gaps and bands of the single-particle band-gap spectrum corresponding to a 2D "square" lattice potential $V_L = V_0[\sin^2(k_l x) + \sin^2(k_l y)]$. Examples of a narrow state density and its phase are shown in Fig. 5. Although the detailed description of such states is beyond the scope of this work, we note that the phase structure displays sharp domain walls associated with strong phase gradients, similar to those in 1D case, which leads to the tight spatial localization of the condensate.

*Conclusions.*—We have demonstrated that, under the conditions of spatially inhomogeneous nonresonant incoherent cw excitation, a polariton condensate can be spatially localized in a periodic in-plane potential owing to the polariton flows established due to the balance between gain and loss. Periodic potential strongly modulates the velocity of the polariton flow out of the pumping region, and the polaritons become self-trapped in the resulting effective potential. This novel mechanism of localization ensures that, depending on the pump intensity, condensate can be formed and localized both in gaps and bands of the single-particle band-gap spectrum of the periodic potential. Localization of the dissipative condensate is therefore irrelevant to the requirement of the negative effective mass which is essential for the gap soliton formation in conservative (atomic) BECs with repulsive interactions [11].

The predicted features of the real-space localization of a dissipative polariton condensate subject to a periodic potential are expected to have strong consequences for any polariton devices incorporating modulated potentials, and should be investigated further.

This work was supported by the Australian Research Council. Discussions with D. Tanese, G. Malpuech, S. Höfling, and A. Kavokin are gratefully acknowledged.

[1] I. Bloch, J. Phys. B **38**, S629 (2005); M. Lewenstein, A. Sanpera, and V. Ahufinger, *Ultracold Atoms in Optical Lattices: Simulating Quantum Many-Body Systems* (Oxford University Press, New York, 2012).

[2] J. Kasprzak, M. Richard, S. Kundermann, A. Baas, P. Jeambrun, J. M. J. Keeling, F. M. Marchetti, M. H. Szymańska, R. André, J. L. Staehli, V. Savona, P. B. Littlewood, B. Deveaud, and Le Si Dang, Nature (London) **443**, 409 (2006).

[3] *Exciton Polaritons in Microcavities, New Frontiers*, Springer Series in Solid-State Sciences Vol. 172, edited by D. Sanvitto and V. Timofeev (Springer, New York, 2012).

[4] C. W. Lai, N. Y. Kim, S. Utsunomiya, G. Roumpos, H. Deng, M. D. Fraser, T. Byrnes, P. Recher, N. Kumada, T. Fujisawa, and Y. Yamamoto, Nature (London) **450**, 529 (2007).

[5] N. Y. Kim, K. Kusudo, C. Wu, N. Masumoto, A. Löffler, S. Höfling, N. Kumada, L. Worschech, A. Forchel, and Y. Yamamoto, Nat. Phys. **7**, 681 (2011).

[6] N. Masumoto, N. Y. Kim, T. Byrnes, K. Kusudo, A. Löffler, S. Höfling, A. Forchel, and Y. Yamamoto, New J. Phys. **14**, 065002 (2012).

[7] D. Tanese, H. Flayac, D. Solnyshkov, A. Amo, A. Lemaître, E. Galopin, R. Braive, P. Senellart, I. Sagnes, G. Malpuech, and J. Bloch, in *Proceedings of the PLMCN12 Conference, Hangzhou, China, 2012*, http://www.physics.fudan.edu.cn/tps/outreach/plmcn12/hangzhouconference/proceeding.html.

[8] E. A. Cerda-Méndez, D. N. Krizhanovskii, M. Wouters, R. Bradley, K. Biermann, K. Guda, R. Hey, P. V. Santos, D. Sarkar, and M. S. Skolnick, Phys. Rev. Lett. **105**, 116402 (2010).

[9] E. A. Cerda-Méndez, D. N. Krizhanovskii, K. Biermann, R. Hey, M. S. Skolnick, and P. V. Santos, New J. Phys. **14**, 075011 (2012).

[10] W. Chen and D. L. Mills, Phys. Rev. Lett. **58**, 160 (1987); Yu. S. Kivshar and G. P. Agrawal, *Optical Solitons: From Fibers to Photonic Crystals* (Academic Press, San Diego, 2003).

[11] H. Pu, L. O. Baksmaty, W. Zhang, N. P. Bigelow, and P. Meystre, Phys. Rev. A **67**, 043605 (2003); B. Eiermann, Th. Anker, M. Albiez, M. Taglieber, P. Treutlein, K.-P. Marzlin, and M. K. Oberthaler, Phys. Rev. Lett. **92**, 230401 (2004); Th. Anker, M. Albiez, B. Eiermann, M. Taglieber, and M. Oberthaler, Opt. Express **12**, 11 (2004); P. J. Y. Louis, E. A. Ostrovskaya, C. M. Savage, and Yu. S. Kivshar, Phys. Rev. A **67**, 013602 (2003); N. K. Efremidis and D. N. Christodoulides, Phys. Rev. A **67**, 063608 (2003); E. A. Ostrovskaya and Yu. S. Kivshar, Opt. Express **12**, 19 (2004).

[12] H. Flayac, D. D. Solnyshkov, and G. Malpuech, Phys. Rev. B **83**, 045412 (2011).

[13] A. V. Gorbach, B. A. Malomed, and D. V. Skryabin, Phys. Lett. A **373**, 3024 (2009).

[14] T. Byrnes, P. Recher, and Y. Yamamoto, Phys. Rev. B **81**, 205312 (2010).

[15] G. Roumpos, W. H. Nitsche, S. Höfling, A. Forchel, and Y. Yamamoto, Phys. Rev. Lett. **104**, 126403 (2010).

[16] J. Keeling and N. G. Berloff, Phys. Rev. Lett. **100**, 250401 (2008).

[17] M. Wouters and I. Carusotto, Phys. Rev. Lett. **99**, 140402 (2007).

[18] E. A. Ostrovskaya, J. Abdullaev, A. S. Desyatnikov, M. D. Fraser, and Yu. S. Kivshar, Phys. Rev. A **86**, 013636 (2012).

[19] G. Roumpos, M. D. Fraser, A. Löffler, S. Höfling, A. Forchel, and Y. Yamamoto, Nat. Phys. **7**, 129 (2011).

[20] E. Wertz, L. Ferrier, D. D. Solnyshkov, R. Johne, D. Sanvitto, A. Lemaître, I. Sagnes, R. Grousson, A. V. Kavokin, P. Senellart, G. Malpuech, and J. Bloch, Nat. Phys. **6**, 860 (2010).

[21] M. Wouters, I. Carusotto, and C. Ciuti, Phys. Rev. B **77**, 115340 (2008).

[22] *Dissipative Solitons*, edited by N. Akhmediev and A. Ankiewicz (Springer, Berlin, 2005).

[23] H. Sakaguchi and B. A. Malomed, Phys. Rev. E **77**, 056606 (2008).

[24] Y. V. Kartashov, V. V. Konotop, V. A. Vysloukh, and L. Torner, Opt. Lett. **35**, 1638 (2010).

[25] See Supplemental Material at http://link.aps.org/supplemental/10.1103/PhysRevLett.110.170407 for more details on localization within the spectral bands.

[26] T. J. Alexander, M. Salerno, E. A. Ostrovskaya, and Yu. S. Kivshar, Phys. Rev. A **77**, 043607 (2008).

[27] T. Anker, M. Albiez, R. Gati, S. Hunsmann, B. Eiermann, A. Trombettoni, and M. K. Oberthaler, Phys. Rev. Lett. **94**, 020403 (2005); T. J. Alexander, E. A. Ostrovskaya, and Yu. S. Kivshar, Phys. Rev. Lett. **96**, 040401 (2006); J. Wang, J. Yang, T. J. Alexander, and Yu. S. Kivshar, Phys. Rev. A **79**, 043610 (2009).